Investigation of a dynamic active/passive noise cancellation of polyborosiloxane thin membrane gel

Konstantinos Myronidis*[a], Gian Piero Malfense Fierro [a], Michele Meo [b], Fulvio Pinto [a]
[a] Department of Mechanical Engineering, University of Bath, Claverton Down, Bath, BA2 7AY, UK
[b] Department of Aeronautics and Astronautics, University of Southampton, Southampton, SO17 1BJ

ABSTRACT

This study proposes a multifunctional, thin membrane gel based on a formulation of PDMS and boron. The proposed gel offers a dynamic passive stimuli-responsive sound absorption at low frequencies, which can be transformed to active noise cancellation with the use of a secondary sound source. The passive behaviour of the proposed material is the result of a dynamic phase transition in the material's polymeric network, activated by the interaction with the travelling sound pressure wave. The presence and extent of the phase transition in the material was investigated via Fourier transform infrared spectroscopy and oscillatory rheological measurements, where it was found that the amount of boron in the gel has a crucial role on the occurrence of the phase transition and consequently on its acoustic performance. The passive scenario results revealed a high and dynamic absorption of approximately 80% at the absorption coefficient peaks, which dynamically shifted to lower frequencies while sound amplitudes were increased. The active noise cancellation was successfully demonstrated at the lower frequencies range, as the occurrence of the phase transition was actively controlled via the sound pressure wave introduced. The aforementioned phase transition was intensified, with energy consumed in this process, resulting in a dynamic noise cancellation. These results demonstrated that the proposed gel membrane material can be used to develop active/passive deep subwavelength absorbers with unique properties, which can dynamically tune their performance in response to external stimuli, and that can be further controlled/activated with the use of mechanical transducers.

*km515@bath.ac.uk

Keywords: Sound absorption, Low Frequency Range, Active/Passive System, Shear Stiffening Gel

1. INTRODUCTION

Noise control has become one of the most significant challenges in an increasing number of engineering applications in the construction, aerospace and railway industries [1, 2], due to the generated discomfort to humans, with the potentiality of becoming harmful over prolonged exposure time periods [3]. In pursuance of sound absorption, research has been focused in a wide range of materials such as composite, recycled and polymeric materials however, environmental, health and energy efficiency concerns have been raised with the use of these [4]. More specifically, the use of natural fibres in composite materials, in an attempt to overcome health concerns rising from synthetic fibres, can only be achieved through energy laborious manufacturing processes, including the use of recycled materials [5]. On the other hand, polymeric materials have been extensively applied in sound absorption applications, however one of their main limitations has been their inability to achieve good sound attenuation performance in the low frequency range [6]. One of the proposed solutions to overcome this issue is that of membrane metamaterial type structures, which makes use of the flapping motion of non-symmetrical rigid platelets [7], nevertheless, due to their performance being dependent on their dimensional and geometrical properties, low frequency sound absorption can only be achieved via greater thicknesses, rendering these unsuitable in applications where dimensional limitations are imposed.

In addition to the aforementioned passive sound absorbers, a hybrid methodology incorporating an active control of its input impedance and resulting in a hybrid active/passive control, has also been proposed by several authors [8, 9]. The primary benefit of such solutions is that the passive sound absorber will absorb the incident sound under medium and high frequencies, while the active one will cancel the low frequency components. These secondary sound sources have been introduced in the form of loudspeakers or piezoelectric actuators positioned in the air cavity behind the passive absorber. Since the first introduction of an electronic sound absorber [10, 11], a wealth of research has been dedicated to such hybrid systems. Elliot et al., [12] investigated several configurations of microphones and loudspeakers of an active hybrid system in an aircraft, pursuing noise reduction derived from the propellers. This active system, which provided feedback to the loudspeakers via a control algorithm, achieved a reduction of up to 13 dB at the fundamental frequency of the propellers at 88 Hz. A control loudspeaker was employed in an impedance tube by Smith et al., [13] as means of active broadband sound absorption system. The loudspeaker made use of a time-based algorithm, which via the input of a microphone enabling impedance-matched sound absorption, achieved broadband attenuation of the incident wave at a frequency range between 100 and 1000 Hz. It is well worth noting that the thickness of the porous material in this study ranged between 12.7 to 50.8 mm and the air cavity from 60 to 120 mm. In a study by Baz [14], the active part of the hybrid methodology focused on tuning the properties of an acoustic metamaterial. The tunable properties of the metamaterial were its effective density and bulk modulus, with the modelling results suggesting that different spatial control of the density, i.e., cells of density A combined with cells of density B, resulting in tailored bulk moduli distributions of these, were in a position to achieve acoustical invincibility.

In the work presented by our group previously [15], an ultrathin (1/618 wavelength) polyborosiloxane-based membrane, successfully achieved high absorption coefficients (>0.9), in the low frequency range. . This polyborosiloxane-based gel demonstrates a similar macro (stiffening) be haviour to that of Shear Thickening Fluids, usually found in literature as Shear Stiffening Gels (SSGs), however, the underlying mechanism enabling this behaviour is significantly dissimilar [16, 17]. SSGs are viscoelastic materials which demonstrate frequency dependent properties, ought to a dynamic phase transition occurrence in their polymeric network. More specifically, SSGs are in a position to autonomously stiffen as a response to an external loading stimulus. The synthesis of these SSGs comprises of the reaction of polydimethylsiloxane (PDMS) and boric or pyroboric acid, resulting in PBDMS. During synthesis, weak electron intermolecular interactions between boron and the oxygen atoms of the siloxane are assembled, resulting in a dynamic boron-oxygen crosslink. The dynamic stiffening behaviour of SSGs is based on the breaking and recovering behaviour of this B-O non-covalent bond [18], exhibiting phase transitions and concurrently displaying excellent energy absorption characteristics. At an equilibrium state, the double polymeric network of polysiloxane backbone and B-O crosslinks will gradually expand, ought to the cold-flow expansion characteristics of the SSG. The application of an external stimulus, i.e., a sound pressure wave, at a low strain rate will impose a phase transition to the gel from its initial state to a viscous regime; in this regime, the polymeric chains have sufficient time to disentangle, which macroscopically results in a rather soft material which can be easily deformed. In a microscopic level, the characteristic breakage time of the B-O bond is shorter than that of the polysiloxane chains, resulting in a certain internal mobility[16, 19]. The

increase of the applied external stimulus to higher strain rates will result in another phase transition, this time from viscous to rubbery state, which macroscopically will give rise to the SSGs stiffness and is responsible for the energy absorption properties of the material. During this diffuse transition, the B-O crosslinks will dynamically break and reform, thus resulting in greater resistance against the disentanglement of the polymeric chains, with these displaying an inability to readjust to dynamic loading conditions [20, 21]. At even higher strain rates another phase transition will occur, this time from a rubbery to a glassy state, with the polymeric chains at this phase organised in groups, appearing as a crystal lattice [22] and failing due to chain rupture.

In this work, a hybrid active/passive methodology is implemented on SSGs, in pursuance of a dynamic noise cancellation in the low frequency range, where the secondary source will act on the material rather than the primary sound source. SSGs have successfully demonstrated their exemplary performance in sound absorption measurements as passive components, with their performance being effectively autonomously tunable to the varying excitation levels these were subjected to. Based on these premises, it is anticipated that an additional excitation source could potentially fully exploit these sound absorption characteristics of SSGs, transforming them to a hybrid active/passive sound absorption system and providing a highly tailorable solution.

2. MATERIALS AND METHODS

2.1 Synthesis of SSG

The synthesis of a polyborosiloxane SSG has been demonstrated in detail from our group in previous research activities [18, 23]. In brief, boric acid was heated to 140 °C for 1 hour and converted to pyroboric acid; Trimethylsiloxy terminated polydimethylsiloxane (PDMS) with a kinematic viscosity of 1K cSt was then used for the synthesis of the SSG, on a stoichiometric ratio of boron to silicon of 1:5. The reagents were homogenized in room temperature in the presence of ethanol and placed in a conventional oven at 180 °C for 72 hours. Upon completion of the reaction, the final product was left to cool in room temperature and collected from the reacting container. All reagents were purchased from Fluorchem UK and used with no further purification.

2.2 Mechanical and Chemical characterisation of SSG

Following the successful synthesis of the SSG, chemical and mechanical characterisation of the material was conducted in order to evaluate the presence of the dynamic crosslinks and evaluate its rate-dependent properties. Fourier Transform infrared spectroscopy (FT-IR) was employed to investigate the conversion of PDMS to a polyborosiloxane-based SSG over a wavenumber between 4000 and 600 cm^{-1}, with a Perkin Elmer FT-IR spectrometer. Oscillatory rheological measurements provided information on the extent of the rate-dependent properties, in terms of storage (G′), loss (G″) moduli and tanδ, over a frequency range between 0.1 and 100 Hz. The rheometer in situ was a TA instruments, DHR-2 rheometer equipped with a 25 mm parallel plate geometry.

2.3 Acoustic Measurements

The sound absorption coefficient α of a material represents the ratio of the total sound energy absorbed by the tested material and expressed as $\boldsymbol{\alpha = 1 - |R^2|}$ **(Eq. 1).** R is the reflection coefficient which in return can be expressed as:

$$\boldsymbol{R = \frac{H_{1,2} - H_I}{H_R - H_{1,2}}\, e[2jk(d + s)]} \qquad \textbf{(Eq. 2)}$$

Where $H_{1,2}$ are transfer functions between the signals of the microphones employed in the measurements, H_I the transfer function of the incident wave, H_R the transfer function of the reflected wave [24], relative to the complex sound pressures captured by the microphones. In addition to these, d is the distance between the two microphones and s the distance between the end of the microphones and the material under examination.

An illustration of the experimental setup employed in the acoustic measurements in this work can be seen in Figure 1.

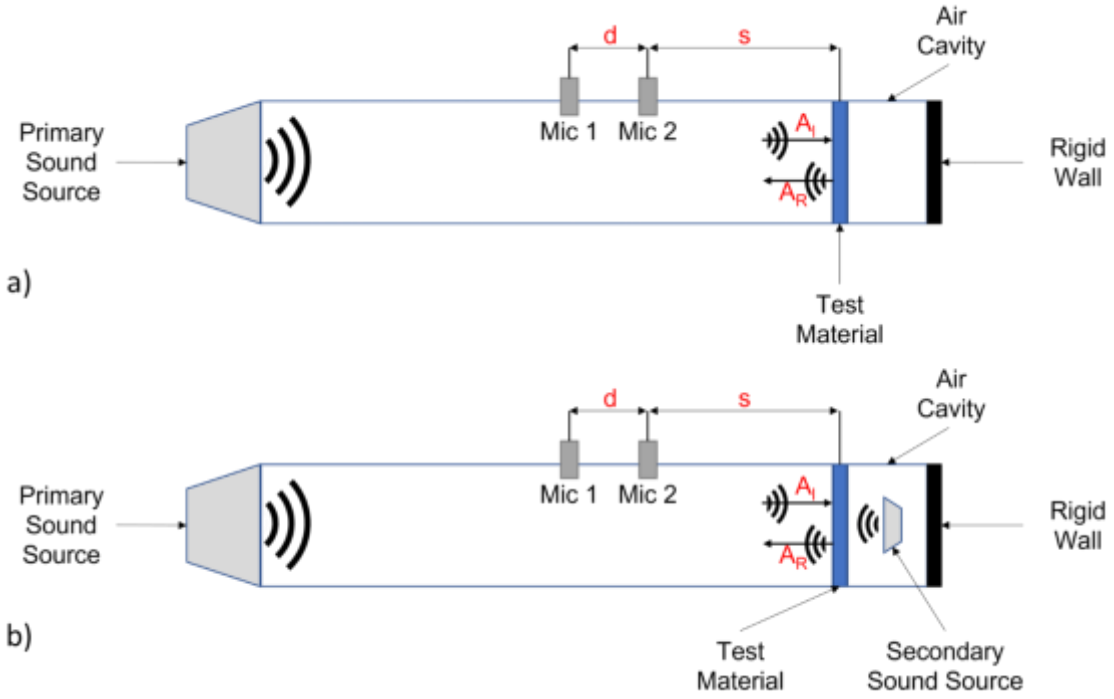

Figure 1 Schematic illustration of apparatus employed in the sound absorption measurements, a) apparatus for passive examination and b) apparatus including a secondary sound source for active examination.

The apparatus consisted of a 50.8 mm aluminium hollow Kundt tube which has been developed in accordance with the ASTM E 1050-07 international standard [25], to provide a standing plane wave propagation inside the tube. The loudspeaker utilised as the primary source sound was a BMS-2592 middle loudspeaker and was used to generate a broadband sweep sinusoidal wave signal, ranging between the lower and upper frequency limits of the apparatus of 200 to 3000 Hz. Two GRAS 40PL 50 Hz-20 kHz, 32-150d B, 10 mV/Pa sensitivity array microphones were positioned inside the Kundt tube, for the measurements of the incident (A_I) and reflected waves (A_R) (Figure 1). An air cavity of 25mm was introduced between the tested sample and the rigid wall at the end of the Kundt tube. The introduction of a mini P5123 loudspeaker in the air cavity behind the tested sample, Figure 1b,with a rated frequency range between 1500 and 45000 Hz and a max sound pressure level of 118 dB, enabled the implementation of the hybrid active/passive methodology. A 3D printed frame was manufactured to mount the secondary sound source. For the sound absorption measurements, SSG samples with a thickness of 1 mm were placed inside a 50.8 mm diameter acrylic ring, with 0.18 mm thickness substrate underneath, to provide a consistent constrain to the polymer, without affecting the performance of the SSG under investigation. The primary source sound was regulated at four different voltage levels of the sweep sinusoidal wave in order to characterise the passive acoustic behaviour of the SSG, as incremental sound pressure loads were applied. The output of the secondary sound source for the active acoustic behaviour of the SSG was controlled via a waveform generator at three excitation frequencies. Both the secondary sound source and the tested samples are depicted in Figure 2 below.

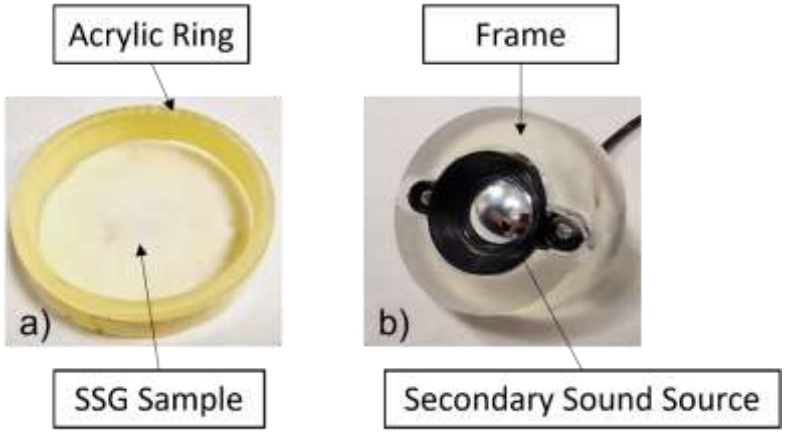

Figure 2 a) SSG sample positioned inside an acrylic ring for sound absorption measurements and b) loudspeaker utilised a secondary sound source positioned inside 3D-printed mount frame.

The geometrical parameters for the sound absorption measurements have been tabulated in Table 1 below.

Table 1 Geometrical arrangements for sound absorption measurements.

Frequency Range	150 – 1000 Hz
Impedance Tube Diameter	50.8 mm
Distance Primary Sound Source – Sample	0 mm
Distance Secondary Sound Source – Sample	330 mm
Distance d	22.5 mm
Distance s	140 mm

3. RESULTS

3.1 Chemical and Mechanical characterisation

The synthesis of the SSG was evaluated both via chemical and mechanical means of characterisation. In Figure 3, the FT-IR spectra of the PDMS precursor and the resulting SSG can be appreciated, providing a qualitative evaluation.

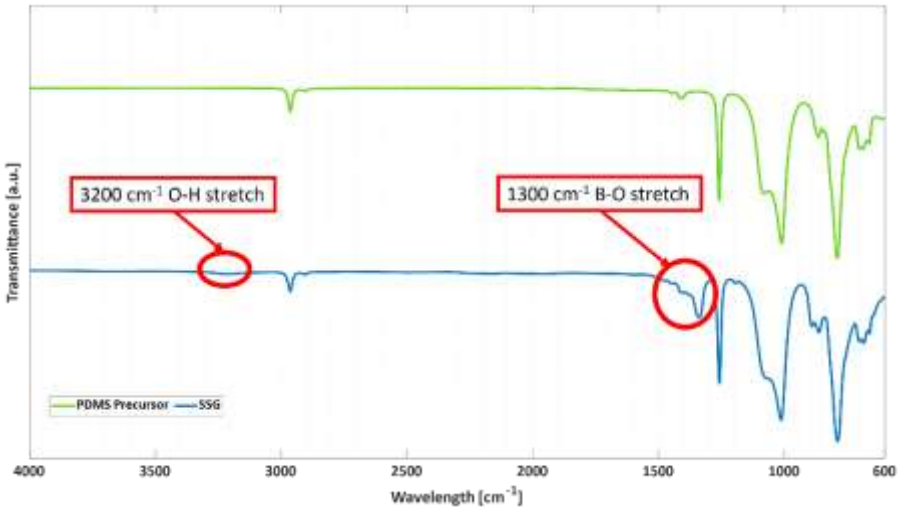

Figure 3 FT-IR Spectra obtained in transmittance from PDMS precursor (green spectra) and SSG (blue spectra) over the examined wavelengths.

In Figure 3, the spectra of the PDMS precursor (green line) and the resulting SSG (blue line) in arbitrary units of transmission are illustrated, over a wavelength range between 4000 and 600 cm^{-1}. As anticipated, the spectra of both materials under investigation demonstrated similarities in their transmittance peaks. More specifically and in good agreement with literature [16, 26, 27], significant peaks were observed at 2900 cm^{-1} (C-H,s) stretch, 1250 cm^{-1} (Si-CH_3,s) stretch, Si-O-Si as stretch and vibrations at 1100 and 1000 cm^{-1}respectively and at 700 cm^{-1} (Si-CH_3,s) stretch. The spectra of the SSG sample diversified from those of its precursor at two significant peaks, the first being at 3200 cm^{-1} (O–H, broad peak) stretch and a broader one in the 1300 cm^{-1} region. [16, 28]. The hydroxy stretching at 3200 cm^{-1} can be attributed to CH_3 groups in the silicon atom, in comparison to the neighbouring signal of 2900 cm^{-1}. For the second diverging region, the peak at 1300 cm^{-1} (B–O, s) stretch, can be considered an important indicator for the successful reaction of the boric acid with the PDMS. Although this peak could be attributed to boric acid or the SSG [27], when considering the hydroxy stretch signal at 3200 cm^{-1} in combination with this peak, it is possible to confer that there is a conversion of the boric acid into the SSG backbone. In addition to this peak, a shoulder at 1380 cm^{-1} can be attributed to B-O-B moieties and the band at 1340 cm^{-1} to Si-O-B moieties, further indicators of the formation of the dynamic network of reversible B-O bonds [16, 27, 28].

In Figure 4, oscillatory rheological measurements of the SSG are illustrated in terms of storage (G′) , loss moduli (G″) and tanδ, over the examined frequencies.

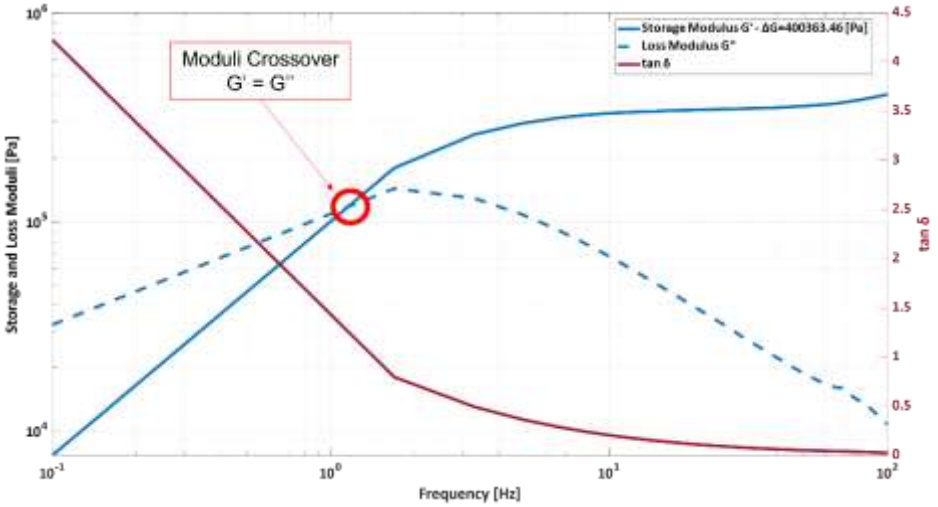

Figure 4 Oscillatory rheological measurements of SSG sample, with G′ (blue line) and G″ (blue dashed line) moduli and tanδ (magenta line) over examined frequencies in logarithmic scales. Moduli crossover (G′=G″) indicated on graph.

The evolution of the curves for the SSG in Figure 4 indicate a material with rate-dependent properties, and more specifically a material with shear stiffening properties. At the beginning of the measured frequencies at 0.1 Hz, G ″ demonstrated higher values compared to G′; in this regime, the viscous properties of the SSG prevail, suggesting that the gel is dissipating energy in the form of heat loss [52]. In this initial state, a small amount of B–O bonds will break and reform, with the polymeric chains having sufficient time to disentangle. Macroscopically the appearance of the SSG in this range of frequencies is of a rather soft and malleable material. The increase of the angular frequencies consequently resulted in an increase to the values of both moduli up to approximately 1.7 Hz where the moduli intersect (G′ = G″). This intersection point is correlated to the phase transition responsible for the energy absorption characteristics of the SSG from viscous to rubbery state, and the occurrence of this point is related to trapped entanglements in the polymeric network of the material, associated to the kinematic viscosity of the PDMS precursor. Past this point, the values of G'' gradually descent, whereas those of G′ ascent and reach a plateau. This diffuse transition induced to the material results in a prevalence of its elastic properties and macroscopically is responsible for the rise of its stiffness and consequently for its energy absorption capabilities. The overall change in G′ for the SSG was approximately 0.4 MPa (from 7.6 kPa to 0.41 MPa) an increase of more than two orders of magnitude. An additional metric of the gel/solid like behaviour of the material is tanδ, with higher values attributed to viscous properties dominated materials, whereas when these approach to zero to solid like materials as tanδ = G″/G′. As can be appreciated from the evolution of this curve, tanδ recorded higher values at the beginning of the measurements, which progressively reduced and approached to zero conferring the moduli measurements. In terms of its acoustic performance, it is anticipated that varying pressure waves will have an analogous effect to that of the rheological measurements to the SSG under investigation, triggering the phase transition and absorbing energy in this process, i.e., an incident sound wave A_I.

3.2 Sound Absorption measurements

For all sound absorption measurements, three repetitions were conducted on each sample and under the same excitation level, with the results hereinafter representing averages of these measurements.

3.2.1 Passive System

In Figure 5, the absorption measurements for the passive system, i.e., primary sound source only, under four different voltage levels of the sweep sinusoidal wave L_{SW}, namely 0.1 mV (orange curve), 2 V (purple curve), 5 V (green curve) and 8 V (blue curve), are illustrated.

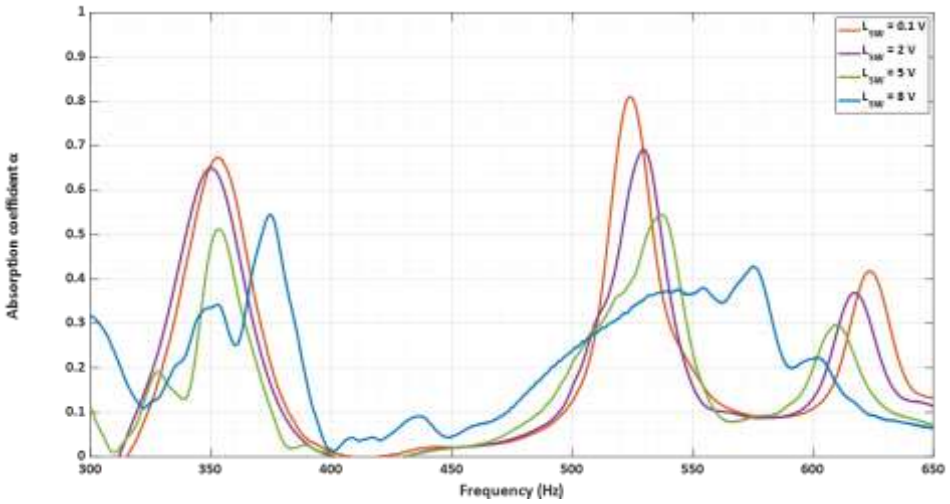

Figure 5 Absorption coefficient measurements of SSG under different voltage levels between 300 – 650 Hz.

Figure 5 represents the absorption coefficients for the different excitation signals from the primary sound source, displaying absorption peaks that occur at a low-frequency range, between 300 and 650 Hz. The occurrence of multiple peaks in this low frequency range has been previously investigated in membrane-type samples synthesised with silicon [29, 30]. In addition to this, a clear shift in the frequency peaks as the voltage level is increased can also be appreciated, with this shift being more evident towards the higher end of the spectrum. More specifically, three regions of high absorption peaks can be identified, in the 352, 523 and 624 Hz regions. In the first region, the average α was evaluated at approximately 0.6, with frequency shifts of 19 Hz across the difference excitation levels. For the second region, that of 523 Hz, the corresponding α was 0.62 and the frequency shift approximately 52Hz. In the final region of 624 Hz, average α was evaluated as 0.38 and the shift towards lower frequencies was in this case approximately 49 Hz. It is well worth noting that at for the highest excitation level, L_{SW} = 8V and blue curve, the peaks have merged between the two regions. All data of interested from the passive system can be found in Table 2.

Table 2 Average absorption frequency peaks evaluated for SSG samples at different voltage levels (σ_α peak $< \pm 0.04$)

Excitation Level	**Frequency [Hz]**	**Absorption Coefficient α**	**Frequency [Hz]**	**Absorption Coefficient α**	**Frequency [Hz]**	**Absorption Coefficient α**
L_{SW} = 0.1 V	352	0.67	523	0.81	624	0.39
L_{SW} = 2 V	358	0.63	530	0.69	617	0.37
L_{SW} = 5 V	353	0.51	537	0.55	610	0.3
L_{SW} = 8 V	373	0.55	575	0.43	575	0.43

3.2.2 Active System

As illustrated in Figure 1b, the apparatus for the active sound absorption measurements methodology utilized the introduction of a secondary sound source in the air cavity behind the SSG under investigation. Prior to the commencement of the active system measurements, the absorption coefficient of the secondary source only were investigated and presented in Figure 6.

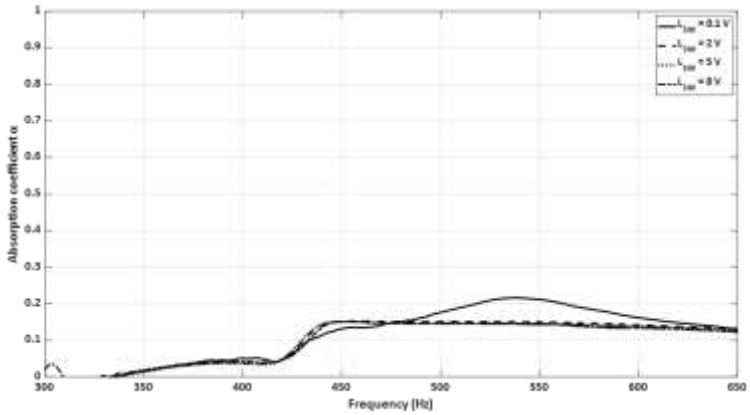

Figure 6 Absorption coefficient measurements of the secondary sound source under different excitation levels of the primary sound source.

As can be appreciated from the curves of the acoustic measurements in Figure 6, the secondary sound source did not provide any sufficient sound cancelation, thus its influence when activated was not significant. Additionally, the excitation levels of the secondary were selected as such (1.5, 3 and 9 kHz) in order to investigate the effect on the stiffening mechanism of the SSG outside the low frequency range between 300 and 650 Hz.

Figure 7 contains sound absorption measurements of the active system under the different excitation levels; continuous lines indicate the passive response of the SSG, dashed lines with the excitation level of the secondary source set at 1.5 kHz, dotted lines at 3 kHz and finally dashed-dotted lines at 9 kHz.

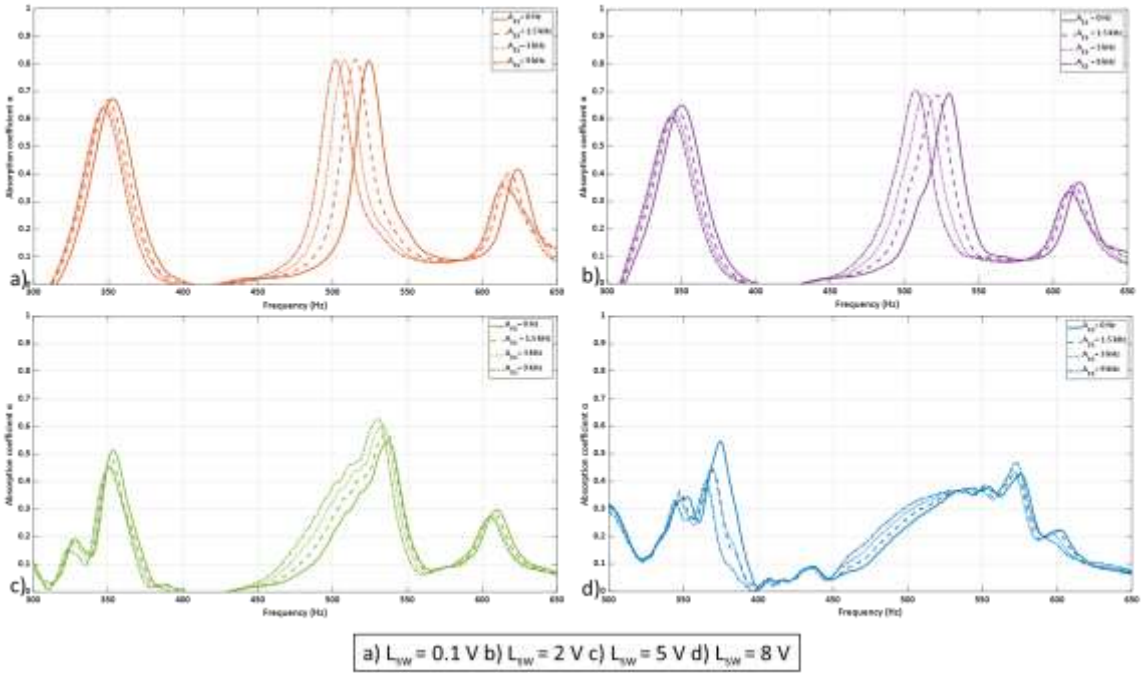

Figure 7 Absorption coefficient measurements of SSG at different excitation levels of primary sound source.

At the lower excitation level of the primary sound source (Figure 7a and L_{SW} = 0.1 V), the evaluated absorption coefficients demonstrated a clear trend observed in similar studies, with a clear shift of these peaks towards lower frequencies [15]. In detail, at the lower frequency range region (352 Hz), α remained virtually unchanged with a shift of frequencies of 10 Hz, whereas the same trend was observed at the higher range (624 Hz), with an approximate α reduction of 10% in this case. The most notable shift occurred in the 523 Hz region, where between the passive and the response at the highest excitation level from the secondary source, a 21 Hz shift was recorded with no reduction to the evaluated sound absorption coefficient. The same behaviour was noted at the second primary source excitation level (Figure 7b and L_{SW} = 2 V), with a small shift on the outer frequency regions of 350 and 617 Hz, and a 21 Hz shift towards lower frequency range between the passive response at this primary source excitation level and the 9 kHz from the secondary sound source. The sound absorption coefficient levels remained on this occasion consistent. Similarly, for the third excitation level (Figure 7c and L_{SW} = 5 V), the shift trend of the absorption coefficient peaks was evident in all three regions, however, α demonstrated an increase of 7% from 0.54 at 537 Hz, to 0.63 at 531 Hz. Finally, as for the passive system, at the higher excitation level of the primary sound source, the two peaks observed in prior measurements in the 523 and 624 Hz region merged, giving way to a more broadband peak at 575 Hz. At this highest level and region, the sound absorption peaks shifted marginally, with this effect being more profound at the lower region of interest, where the overall shift was approximately 10 Hz. The same information can be further appreciated in Figure 8, where the sound absorption coefficient peaks are compared across the excitation from the secondary sound source, where Figure 8a is A_{ES} = 1.5 kHz, Figure 8b is A_{ES} = 3 kHz and Figure 8c is A_{ES} = 9 kHz

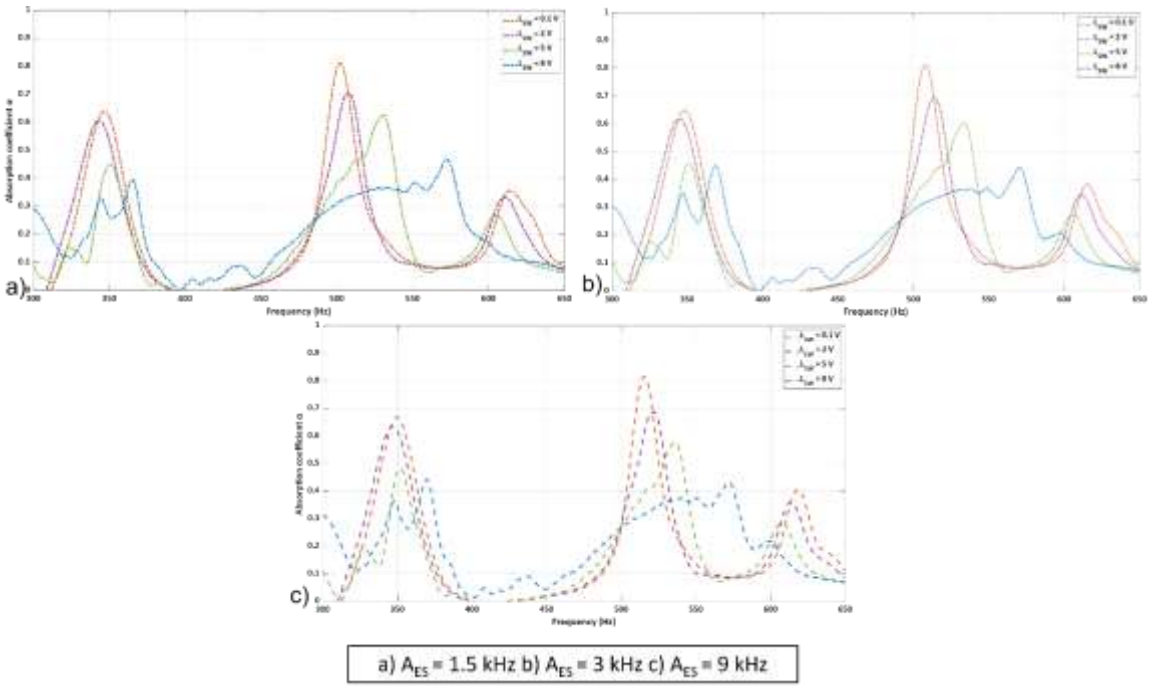

Figure 8 Absorption coefficient measurements of SSG at different excitation levels of secondary sound source.

All data across the different regions of interest, i.e., 352, 523 and 624 Hz, from the active system have been tabulated in Table 3, Table 4 and Table 5.

Table 3 Average absorption frequency peaks evaluated for SSG samples at different voltage levels for passive and active system in frequency range of interest of 352 Hz (σ_α peak < ± 0.02)

	Frequency [Hz]	Absorption Coefficient α	Frequency [Hz]	Absorption Coefficient α	Frequency [Hz]	Absorption Coefficient α	Frequency [Hz]	Absorption Coefficient α
Passive System	**L_{SW} = 0.1 V**		**L_{SW} = 2 V**		**L_{SW} = 5 V**		**L_{SW} = 8 V**	
	352	0.67	350	0.65	353	0.51	375	0.55
A_{ES} = 1.5 kHz	349	0.67	346	0.63	352	0.48	369	0.44
A_{ES} = 3 Hz	348	0.65	345	0.62	351	0.46	369	0.45
A_{ES} = 9 kHz	346	0.64	343	0.61	350	0.45	365	0.40

Table 4 Average absorption frequency peaks evaluated for SSG samples at different voltage levels for passive and active system in frequency range of interest of 523 Hz (σα peak < ± 0.02)

	Frequency [Hz]	Absorption Coefficient α	Frequency [Hz]	Absorption Coefficient α	Frequency [Hz]	Absorption Coefficient α	Frequency [Hz]	Absorption Coefficient α
Passive System	**L_{SW} = 0.1 V**		**L_{SW} = 2 V**		**L_{SW} = 5 V**		**L_{SW} = 8 V**	
	523	0.81	530	0.69	537	0.55	575	0.43
A_{ES} = 1.5 kHz	515	0.81	521	0.69	536	0.58	571	0.43
A_{ES} = 3 kHz	509	0.81	514	0.69	534	0.60	571	0.44
A_{ES} = 9 kHz	502	0.81	508	0.70	531	0.63	572	0.47

Table 5 Average absorption frequency peaks evaluated for SSG samples at different voltage levels for passive and active system in frequency range of interest of 624 Hz (σα peak < ± 0.02)

	Frequency [Hz]	Absorption Coefficient α	Frequency [Hz]	Absorption Coefficient α	Frequency [Hz]	Absorption Coefficient α	Frequency [Hz]	Absorption Coefficient α
Passive System	**L_{SW} = 0.1 V**		**L_{SW} = 2 V**		**L_{SW} = 5 V**		**L_{SW} = 8 V**	
	624	0.42	617	0.37	610	0.3	575	0.43
A_{ES} = 1.5 kHz	618	0.40	614	0.36	608	0.28	571	0.43
A_{ES} = 3 kHz	615	0.38	611	0.35	606	0.27	571	0.44
A_{ES} = 9 kHz	613	0.35	610	0.33	605	0.27	572	0.47

4. DISCUSSION

The main concept of the PBS-based SSG in this work was to exploit its dynamic change in stiffness, owed to a diffuse transition from viscous to rubbery state. It was anticipated that the presence of an additional sound source would enhance its stiffening characteristics, which in return would result in more profound and tailored sound absorption characteristics to the needs of a specific application. The chemical characterisation of the material established the presence of the dynamic B-O bonds in its polymeric network, which are responsible for its excellent energy absorption characteristics. The mechanical characterisation, via means of rheological measurements, demonstrated the rate dependency of this effect and also provided a quantitative measurement. During the sound absorption measurements on a passive system (Figure 1a), a clear shift in absorption coefficient peaks was observed towards higher frequencies, across various excitation levels; this occurrence can be attributed to the stiffening effect of the polyborosiloxane-based SSG material, which was induced as the external stimulus, on this occasion the sound pressure wave of the primary sound source increased. Once this stimulus was applied on the SSG, the diffuse transition in the polymeric network of the material resulted in energy absorbed for the dynamic breaking and reformation of the supramolecular B-O network. The acoustic properties of the material underwent a dynamic change, since these are highly affected by the dynamic transport parameters such as permeability and tortuosity, in addition to morphology of the polymeric network and thermal-dependent parameters [31-33]. The uniqueness of each formulation of the SSGs, ought to the PDMS precursor employed and the environmental conditions during the synthesis, appeared to have a direct effect on the position, amplitude and shift of the sound absorption coefficient peaks, when these are compared to previous studies [15].

The introduction of a secondary sound source in the sound absorption measurements (Figure 1b), yielded the anticipated results. An adaptive behaviour relative to the second excitation signal was demonstrated, evident by the shift of the absorption peaks towards lower frequencies. The presence of an active system led to a more efficient stiffening effect in the polymeric network of the SSG and a more pronounced shift towards lower frequencies. Considering that the tested material was synthesised from the same precursor, its adaptive behaviour can only attributed in the dynamic breaking and reformation of the B-O supramolecular network. Although that in the passive system a decrease in the amplitude of the peaks was recorded, this was not held true for all peaks in the active system. The high sound absorption coefficients achieved (>0.8) suggest that the SSG under investigation is in a position to absorb great amounts of incident energy. More importantly though, the frequency range of the achieved sound absorption can be tuned via a secondary source, further corroborating the dynamic energy absorption characteristics of the SSG and their unique tuneable characteristics.

5. CONCLUSIONS

In conclusion, a polyborosiloxane-based SSG is proposed in this work, which is able to achieve high sound absorption coefficient (>0.8) at specific frequencies in a passive system and when it was introduced into an active system maintain and further intensify this dynamic shift towards lower frequencies. This frequency shift derived from the unique stiffening effect of the material, which was primarily demonstrated in the oscillatory rheological measurements. This stiffening effect led to dynamic shifts of 19, 52 and 49 Hz of the absorption frequency peaks, with these occurring in a low frequency range between 350 and 610 Hz. The frequency shift was ought to the dynamic transition of the material from a viscous to a rubbery state, with the amount of the energy absorbed by the dynamic B-O network was increased proportionally to the increase of the excitation level. The introduction of a secondary excitation source resulted in a further shift of the absorption peaks towards lower frequencies, indicating that the stiffening effect in the supramolecular network of the SSG was further exploited.

The results indicate that the SSG membranes presented in this study are in a position to achieve relatively high, and more importantly greatly adaptive sound absorption performance, when a secondary excitation source is introduced in the system, This unique performance is evident in the low frequency range and can be achieved with deep subwavelength thicknesses (up to 1/618 wavelength) in contrast to traditional acoustic materials. The SSG membranes in this study are able to offer an efficient alternative in noise control applications in a wide range of engineering industries, where spatial limitations are in situ and low-frequency cancelation is required.

FUNDING

The work in this publication was conducted under the project with title “Aegis, Advanced Energy-Absorption Polymer for Impact-Resistant Smart Composites” funded by the Engineering and Physical Sciences Research Council [EP/T000074/1].

REFERENCES

[1] C.H. Hansen, K.L. Hansen, Noise control: from concept to application, CRC Press2021.
[2] G. Müller, M. Möser, Handbook of engineering acoustics, Berlin : Springer, Berlin, 2013.
[3] S.Q. Hu, W.J. Hu, S. Yang, X.H. Zhu, K. Sun, S.S. Jiang, Y.X. Qiu, X.D. Li, [Investigation on noise exposure level and health status of workers in transportation equipment manufacturing industry], Zhonghua Lao Dong Wei Sheng Zhi Ye Bing Za Zhi 39(7) (2021) 498-502.
[4] C.A. Echeverria, F. Pahlevani, W. Handoko, C. Jiang, C. Doolan, V. Sahajwalla, Engineered hybrid fibre reinforced composites for sound absorption building applications, Resources, Conservation and Recycling 143 (2019) 1-14.
[5] S.V. Joshi, L. Drzal, A. Mohanty, S. Arora, Are natural fiber composites environmentally superior to glass fiber reinforced composites?, Composites Part A: Applied science and manufacturing 35(3) (2004) 371-376.
[6] T.L. Yang, D.-M. Chiang, R. Chen, Development of a novel porous laminated composite material for high sound absorption, Journal of Vibration and Control 7(5) (2001) 675-698.
[7] J. Mei, G. Ma, M. Yang, Z. Yang, W. Wen, P. Sheng, Dark acoustic metamaterials as super absorbers for low-frequency sound, Nature Communications 3(1) (2012) 756.
[8] M. Furstoss, D. Thenail, M.A. Galland, SURFACE IMPEDANCE CONTROL FOR SOUND ABSORPTION: DIRECT AND HYBRID PASSIVE/ACTIVE STRATEGIES, Journal of Sound and Vibration 203(2) (1997) 219-236.
[9] M.-A. Galland, B. Mazeaud, N. Sellen, Hybrid passive/active absorbers for flow ducts, Applied Acoustics 66(6) (2005) 691-708.
[10] H.F. Olson, E.G. May, Electronic sound absorber, The Journal of the Acoustical Society of America 25(6) (1953) 1130-1136.
[11] P. Lueg, Process of silencing sound oscillations, US pat ent 2043416 (1936).
[12] S.J. Elliot, P.A. Nelson, I.M. Stothers, C.C. Boucher, In-flight experiments on the active control of propeller-induced cabin noise, Journal of Sound and Vibration 140(2) (1990) 219-238.
[13] J.P. Smith, B.D. Johnson, R.A. Burdisso, A broadband passive–active sound absorption system, The Journal of the Acoustical Society of America 106(5) (1999) 2646-2652.
[14] A.M. Baz, An active acoustic metamaterial with tunable effective density, Journal of vibration and acoustics 132(4) (2010).
[15] M. Boccaccio, K. Myronidis, M. Thielke, M. Meo, F. Pinto, A multifunctional ultra-thin acoustic membrane with self-healing properties for adaptive low-frequency noise control, Scientific Reports 12(1) (2022) 17790.
[16] Z. Liu, S.J. Picken, N.A. Besseling, Polyborosiloxanes (PBSs), synthetic kinetics, and characterization, Macromolecules 47(14) (2014) 4531-4537.
[17] F. Pinto, M. Meo, Design and Manufacturing of a Novel Shear Thickening Fluid Composite (STFC) with Enhanced out-of-Plane Properties and Damage Suppression, Applied Composite Materials 24(3) (2017) 643-660.
[18] K. Myronidis, M. Thielke, M. Kopeć, M. Meo, F. Pinto, Polyborosiloxane-based, dynamic shear stiffening multilayer coating for the protection of composite laminates under Low Velocity Impact, Composites Science and Technology 222 (2022) 109395.
[19] N. Seetapan, A. Fuongfuchat, D. Sirikittikul, N. Limparyoon, Unimodal and bimodal networks of physically crosslinked polyborodimethylsiloxane: viscoelastic and equibiaxial extension behaviors, Journal of Polymer Research 20(7) (2013) 1-9.
[20] X. Li, D. Zhang, K. Xiang, G. Huang, Synthesis of polyborosiloxane and its reversible physical crosslinks, Rsc Advances 4(62) (2014) 32894-32901.
[21] S. Zhang, S. Wang, T. Hu, S. Xuan, H. Jiang, X. Gong, Study the safeguarding performance of shear thickening gel by the mechanoluminescence method, Composites Part B: Engineering 180 (2020) 107564.

[22] W. Jiang, X. Gong, S. Wang, Q. Chen, H. Zhou, W. Jiang, S. Xuan, Strain rate-induced phase transitions in an impact-hardening polymer composite, Applied Physics Letters 104(12) (2014) 121915.
[23] K. Myronidis, M. Boccaccio, M. Meo, F. Pinto, Multifunctional, Smart, Non-Newtonian Polymer Matrix with Improved Anti-impact Properties Enabling Structural Health Monitoring in Composite Laminates, European Workshop on Structural Health Monitoring, Springer, 2023, pp. 844-855.
[24] D.-Y. Maa, Microperforated-Panel Wideband Absorbers, Noise Control Engineering Journal 29(3) (1987) 77-84.
[25] A.S.f. Testing, Materials, ASTM E 1050-07. Standard Test Method for Impedance and Absorption of Acoustical Materials Using a Tube, Two Microphones and a Digital Frequency Analysis System, Westcohocken, PA ASTM, 2007.
[26] A. Mata, A.J. Fleischman, S. Roy, Characterization of polydimethylsiloxane (PDMS) properties for biomedical micro/nanosystems, Biomedical microdevices 7 (2005) 281-293.
[27] G. Zinchenko, V. Mileshkevich, N. Kozlova, Investigation of the synthesis and hydrolytic degradation of polyborodimethylsiloxanes, Polymer Science USSR 23(6) (1981) 1421-1429.
[28] F.V. Drozdov, S.A. Milenin, V.V. Gorodov, N.V. Demchenko, M.I. Buzin, A.M. Muzafarov, Crosslinked polymers based on polyborosiloxanes: Synthesis and properties, Journal of Organometallic Chemistry 891 (2019) 72-77.
[29] F. Bucciarelli, M. Meo, Broadening sound absorption coefficient with hybrid resonances, Applied Acoustics 160 (2020) 107136.
[30] F. Bucciarelli, G.P. Malfense Fierro, M. Meo, A multilayer microperforated panel prototype for broadband sound absorption at low frequencies, Applied Acoustics 146 (2019) 134-144.
[31] J. Allard, N. Atalla, Propagation of sound in porous media: modelling sound absorbing materials 2e, John Wiley & Sons2009.
[32] D.J. Oldham, C.A. Egan, R.D. Cookson, Sustainable acoustic absorbers from the biomass, Applied Acoustics 72(6) (2011) 350-363.
[33] S. Ren, F. Xin, T.J. Lu, C. Zhang, A semi-analytical model for the influence of temperature on sound propagation in sintered metal fiber materials, Materials & Design 134 (2017) 513-522.